Table III. Calculated One-, Two-, and Three-Center Contributions to HFI Tensors of ^{14}N in $Cu(mnt)_2^{2-}$ and $Cu(Et_2dtc)_2$ and the Experimentally Determined Tensors (in MHz)

	one center	two and three center	one, two, and three center	exptl
			dtc-EH[a]	
A_x	−0.03	0.15	0.12	0.18
A_y	0.06	−0.03	0.03	0.18
A_z	−0.03	−0.12	−0.15	−0.36
A_{iso}	0.0	0.0	0.0	−1.124
			dtc-UHFS[b]	
A_x	0.24	0.15	0.39	0.18
A_y	0.48	−0.03	0.45	0.18
A_z	−0.72	−0.12	−0.84	−0.36
A_{iso}	−1.68	0.0	−1.68	−1.124
			mnt N(1)	
A_1	−0.471	0.156	−0.315 (24, x)	−0.318 (34, x)
A_2	−0.477	−0.009	−0.483 (11, z)	−0.486 (25, z)
A_3	0.948	−0.147	0.798 (26, y)	0.804 (24, y)
A_{iso}	0.126	0.051	0.177	0.306
			N(2)	
A_1	−0.420	0.147	−0.273 (21, x)	−0.249 (41, x)
A_2	−0.426	−0.012	−0.435 (9, z)	−0.471 (27, z)
A_3	0.846	−0.135	0.708 (157, y)	0.720 (151, y)
A_{iso}	0.123	0.051	0.174	0.231

[a] One-center interaction calculated from extended Hückel coefficients. [b] One-center interaction calculated from spin densities obtained with an unrestricted Hartree–Fock–Slater calculation.[35]

be nonaxial. This is in agreement with the experiment. The total results for the anisotropic parts are equal to the experimental tensors, both in magnitude and direction, a result that might be fortuitous on the basis of the very crude MO method used. The calculated isotropic HFI is ~50% of the experimental value.

The calculated quadrupole tensors are listed in Table I. Taking into account the approximations in this calculation[34] (only one-center electric field gradient contributions; no lattice contribution) the result is satisfactory: the directions fit the experiment; the principal values are ~50% too large.

Conclusions

In conclusion we can state that the following:

1. The hyperfine and the quadrupole interaction can be measured very accurately, notwithstanding the fact that the spectra are very complicated due to the presence of two nonequivalent nitrogen atoms and the fact that all the interactions are small (i.e. not larger than 2 MHz).
2. The simulation of the ESEEM spectra is remarkably successful, considering the presence of two nitrogen spins. The suppression effect is taken into account by substituting the experimental value of τ in formula 3.
3. The observed splittings of the lines in certain directions of the magnetic field are not understood.
4. The MO calculation gives insight into the electronic structure of the molecule. The agreement between the calculated and the experimental tensors is very satisfactory, especially considering the approximate nature of the MO method.

Acknowledgment. We thank Professor E. de Boer for critically reading the manuscript and stimulating discussions. We are also very grateful to Dr. T. Weeding for correcting the English text.

Registry No. $(n\text{-}Bu_4N)_2(I)$, 15077-49-3; $(NBu_4)_2Ni(mnt)_2$, 18958-57-1.

Contribution from the Istituto di Chimica Generale ed Inorganica, Università di Torino, 10125 Torino, Italy, and Dipartimento di Chimica Inorganica e Metallorganica, Università di Milano, 20133 Milano, Italy

Vibrational Studies of Interstitial Carbide Atoms in Nickel and Rhenium Carbonyl Carbide Clusters

P. L. Stanghellini,*† R. Rossetti,† G. D'Alfonso,‡ and G. Longoni‡

Received May 16, 1986

A vibrational spectroscopy study of the interstitial carbon atom in a series of Re and Ni carbide clusters enabled the M–C vibrational modes to be assigned and the effect of the metal atoms capping the $Re_6(\mu_6\text{-}C)$ and $Ni_8(\mu_8\text{-}C)$ cores to be investigated. The assignment of the M–C vibrational modes has been confirmed by ^{13}C isotopic labeling of the interstitial carbide atom. A single force constant value accounts for the observed frequencies in the nickel carbide clusters, whether capped or uncapped, and in the uncapped rhenium carbide clusters. In contrast, the vibrational analysis for the capped rhenium clusters indicates that the force field around the carbon atom should be described by slightly different axial and equatorial force constants. A rationalization of the capping effect in terms of structural and electronic effects is proposed.

Introduction

Transition-metal carbide clusters have received wide attention in the last decade, probably because of their possible implications with carbon atoms either adsorbed or nested on a metal surface or encapsulated in a metal lattice. As a result, there are now examples of carbide clusters of several transition metals, e.g. Re, Fe, Ru, Os, Co, Rh, and Ni, in which the carbon atom shows a wide spectrum of coordination ranging from μ_4 to μ_8.[1-3]

Since the first complete assignment of the M–C vibrational modes,[4,5] several reports on the vibrational spectra of exposed, semiinterstitial, and interstitial carbide clusters have appeared.[6-12] In the case of interstitial carbide clusters only the octahedral, e.g. $[Fe_6C(CO)_{16}]^{2-}$, $[Ru_6C(CO)_{16}]^{2-}$,[12] and $[Os_{10}C(CO)_{24}]^{2-}$,[7] and trigonal-prismatic, e.g. $Co_6C(CO)_{12}(\mu_3\text{-}S)_2$,[4,5] $[Co_6C(CO)_{15}]^{2-}$, and $[Rh_6C(CO)_{15}]^{2-}$,[10] coordinations of carbon have received

† Università di Torino.
‡ Università di Milano.

(1) Tachikawa, M.; Muetterties, E. L. *Prog. Inorg. Chem.* **1981**, *28*, 301.
(2) Albano, V. G.; Martinengo, S. *Nachr. Chem., Tech. Lab.* **1980**, *28*, 654.
(3) Bradley, J. S. *Adv. Organomet. Chem.* **1983**, *22*, 1.
(4) Bor, G.; Stanghellini, P. L. *J. Chem. Soc., Chem. Commun.* **1979**, 886.
(5) Bor, G.; Dietler, U. K.; Stanghellini, P. L.; Gervasio, G.; Rossetti, R.; Sbrignadello, G.; Battiston, G. A. *J. Organomet. Chem.* **1981**, *213*, 277.
(6) Oxton, I. A.; Powell, D. B.; Farrar, D. M.; Johnson, B. F. G.; Lewis, J.; Nicholls, S. N. *Inorg. Chem.* **1981**, *20*, 4302.
(7) Oxton, I. A.; Kettle, S. F. A.; Jackson, P. F.; Johnson, B. F. G.; Lewis, J. *J. Mol. Struct.* **1981**, *71*, 117.
(8) Oxton, I. A.; Powell, D. B.; Goudsmith, R. J.; Johnson, B. F. G.; Lewis, J.; Nelson, W. J. H.; Nicholls, J. N.; Rosales, M. S.; Vargas, M. D.; Whitmire, K. H. *Inorg. Chim. Acta* **1982**, *64*, L259.
(9) Johnson, B. F. G.; Lewis, J.; Nicholls, J. N.; Owton, I. A.; Raithby, P. R.; Rosales, M. *J. Chem. Soc., Chem. Commun.* **1982**, 289.
(10) Creghton, J. A.; Della Pergola, R.; Heaton, B. T.; Martinengo, S.; Strona, L.; Willis, D. A. *J. Chem. Soc., Chem. Commun.* **1982**, 864.

0020-1669/87/1326-2769$01.50/0

attention. Although the square-antiprismatic coordination of carbon is commonly found in binary metal carbides, e.g., $Cr_{23}C_3$,[13] there have been no reports of corresponding studies on square-antiprismatic carbide clusters. Furthermore, with the aim of gaining a better understanding of the interactions of the encapsulated carbide atom with the surrounding metal atoms, it was of interest to investigate the effect of progressive capping of the metal frame originating the cage.

The recently isolated and characterized Ni and Re clusters give such an opportunity both for an octahedral and for a square-antiprismatic metal frame, and here we report the results of vibrational studies of $[NMe_4]_2[Ni_8C(CO)_{16}]$ (I), $[NMe_4]_2[Ni_9C(CO)_{17}]$ (II), $[NMe_4][Ni_{10}C(CO)_{18}]$ (III), $[NEt_4]_2[Re_8C(CO)_{24}]$ (IV), $[NEt_4]_5\{[Re_7AgC(CO)_{21}]_2\}$ (V), $[NEt_4]_3[Re_7C(CO)_{21}]$ (VI), $[NEt_4][Re_7C(CO)_{21}(\mu\text{-CO})]$ (VII), $[NEt_4]_2[Re_6C(CO)_{18}(H)_2]$ (VIII), and $[NEt_4]_2[Re_6C(CO)_{18}(\mu\text{-CO})]$ (IX).

Experimental Part

Syntheses. The Ni carbide clusters have been prepared by literature methods.[14] The compounds ^{13}C selectively labeled at the carbide atom were prepared by using $^{13}CCl_4$ (94.3%) from MSD Isotopes.

Detailed reports deal with the syntheses of the Re clusters IV,[15] V,[16] VI,[17] VII,[18] VIII,[19] and IX.[18] The ^{13}C-enriched samples of IV and VI were obtained by pyrolysis of ca. 20% ^{13}CO-enriched $[NEt_4][ReH_2(CO)_4]$.

IR Spectra. The infrared spectra were recorded by means of a 580B Perkin-Elmer grating spectrophotometer and elaborated, when necessary, by a 1200 Data Station with the provided PE 580 software. The spectra were obtained on samples of KBr and CsI disks either at ca. 300 K or at ca. 110 K, with the use of a special vacuum IR cell cooled with liquid nitrogen.

Force Constant Calculation. The approximate values of the M–C force constants have been calculated by the **FG** Wilson method,[20] using a complete **G** matrix and a diagonal **F** matrix. This corresponds to a simple valence force field approximation in which any coupling is neglected between M–C coordinates with other coordinates such as M–M stretch and M–CO strech and deformation. In other words, the M–C vibrations are regarded as motions of the interstitial carbide in an infinitely heavy metal cage. The **G** matrix elements were calculated on the basis of the idealized symmetry of the metal cage, whose geometrical center is occupied by the carbide atom, by using, as internal coordinates, the stretch of the formal M–C bonds. The actual structures show small deviations (5% or less) from the idealized symmetry, which does not significantly affect the results.

The values of the **G** matrix elements of the M–C modes are the following.

(i) Ni Systems. Complex I (symmetry D_{4d}): $G(B_2) = (8/m_c)(\cos\alpha)$; $G(E_1) = (4/m_c)(1 - \cos\alpha)$. Complex II (symmetry C_{4v}): $G(A_1) = (8/m_c)(\cos\alpha)$; E block, $G_{11} = G_{22} = (2/m_c)(2^{1/2} - 1)(1 - \cos\alpha)$, $G_{33} = G_{44} = (2^{1/2} - 1)/(2^{1/2} + 1)G_{11}$, $G_{14} = -G_{23} = (G_{11}G_{33})^{1/2}$, $G_{12} = G_{13} = G_{24} = G_{34} = 0$ (α is the NiCNi angle in which both Ni atoms belong to the same square face).

(ii) Re Systems. Complex IV (symmetry D_{3d}): $G(A_{2u}) = (2/m_c)(1 + 2\cos\alpha)$; $G(E_u) = (2/m_c)(1 - \cos\alpha)$. Complexes V and VI (symmetry C_{3v}); A_1 block, $G_{11} = (1/m_c)(1 + 2\cos\alpha)$, $G_{22} = (1/m_c)(1 + 2\cos\beta)$, $G_{12} = -(G_{11}G_{22})^{1/2}$; E block, $G_{11} = G_{22} = (1/m_c)(1 - \cos\alpha)$, $G_{33} = G_{44} = (1/m_c)(1 - \cos\beta)$, $G_{23} = G_{34} = -(G_{11}G_{33})^{1/2}$, $G_{12} = G_{14} = G_{23} = G_{34} = 0$ (α and β are the ReCRe and Re′CRe′ angles, respectively, in which Re atoms belong to the Re-capped Re_3 triangle and Re′ atoms belong to the Ag-capped (V) or uncapped (VI) Re_3 triangle).

Table I. Observed (Calculated) Frequency Values (cm^{-1}) of ν(M–C) Modes

		mode	^{12}C	^{13}C
I	$[Ni_8C(CO)_{16}]^{2-}$	B_2	524 (529)	n.d. (508)
		E	580 (579)	557 (556)
II	$[Ni_9C(CO)_{17}]^{2-}$	A_1	522 (523)	506 (503)
		E	582 (581)	560 (558)
III	$[Ni_{10}C(CO)_{18}]^{2-}$	E_1[a]	584	
IV	$[Re_8C(CO)_{24}]^{2-}$	A_{2u}	655 (654)	637 (629)
		E_u	696 (696)	670 (669)
V	$[Re_7AgC(CO)_{21}]^{2-}$	A_1	635	
		E	678	
VI	$[Re_7C(CO)_{21}]^{3-}$	A_1	662 (662)	640 (636)
		E	688 (689)	662 (662)
VII	$[Re_7C(CO)_{21}(\mu\text{-CO})]^-$	A′	695 (698)	
		A′	670	
		A″	685 (682)	
VIII	$[Re_6C(CO)_{18}(H)_2]^{2-}$	$A_2 + E$	690	
IX	$[Re_6C(CO)_{18}(\mu\text{-CO})]^{2-}$		678	
			660	

[a] For a presumable D_{4d} symmetry.

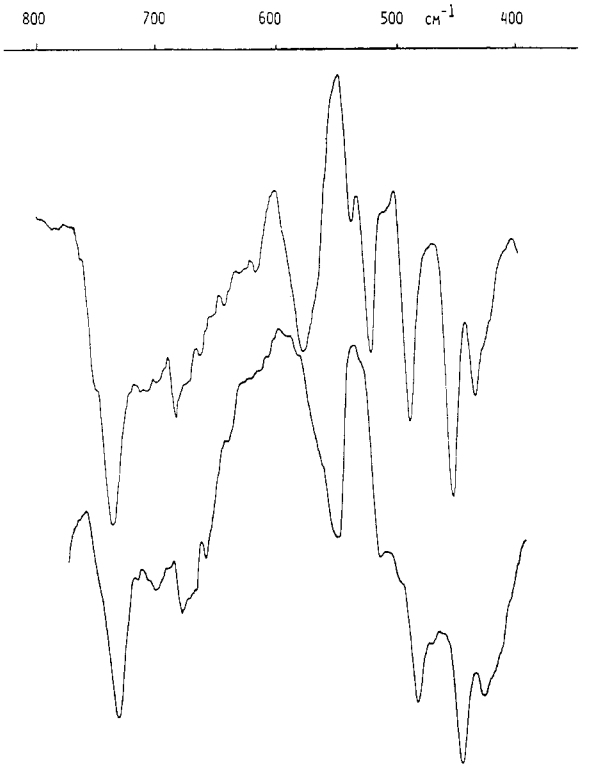

Figure 1. IR spectra of complex I in a CsI disk at ca. 110 K: upper curve, ^{12}C compound; lower curve, ^{13}C compound.

Results

(a) Complexes I–III. The metal core structure of I is a slightly distorted square antiprims with idealized D_{4d} symmetry, from which that of II is ideally derived by capping a square face with

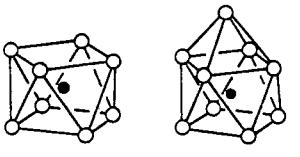

I II

an Ni atom, to obtain C_{4v} symmetry. In both cases the carbide atom occupies the center of the core and its vibrational degrees of freedom span a double degenerated E mode and a nondegen-

(11) Kolis, J. W.; Basolo, F.; Shriver, D. F. *J. Am. Chem. Soc.* **1982**, *104*, 5626.
(12) Stanghellini, P. L.; Cognolato, L.; Bor, G.; Kettle, S. F. A. *J. Crystallogr. Spectrosc. Res.* **1983**, *13*, 127.
(13) Bowman, A. L.; Arnold, G. P.; Storms, E. K.; Neresov, N. G. *Acta Crystallogr., Sect. B: Struct. Crystallogr. Cryst. Chem.* **1972**, *B28*, 3102.
(14) Ceriotti, A.; Longoni, G.; Manassero, M.; Perego, M.; Sansoni, M. *Inorg. Chem.* **1985**, *24*, 117.
(15) Ciani, G.; D'Alfonso, G.; Freni, M.; Romiti, P.; Sironi, A. *J. Chem. Soc., Chem. Commun.* **1982**, 705.
(16) Beringhelli, T.; D'Alfonso, G.; Freni, M.; Ciani, G.; Sironi, A. *J. Organomet. Chem.* **1985**, *295*, C7.
(17) Ciani, G.; D'Alfonso, G.; Freni, M.; Romiti, P.; Sironi, A. *J. Chem. Soc., Chem. Commun.* **1982**, 339.
(18) Beringhelli, T.; D'Alfonso, G.; Ciani, G.; Sironi, A. manuscript in preparation.
(19) Ciani, G.; D'Alfonso, G.; Romiti, P.; Sironi, A.; Freni, M. *J. Organomet. Chem.* **1983**, *244*, C27.
(20) Wilson, E. B., Jr.; Decius, J. C.; Cross, P. C. *Molecular Vibrations*; Dover: New York, 1980.

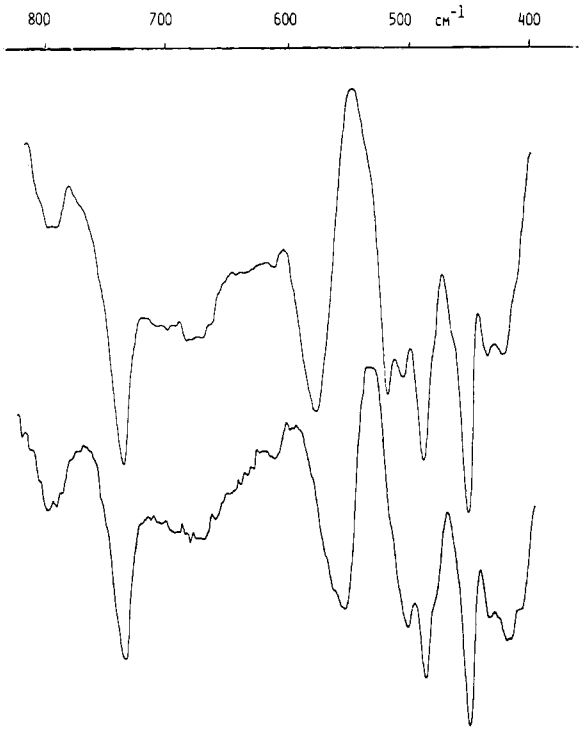

Figure 2. IR spectra of complex II in a CsI disk at ca. 110 K: upper curve, ^{12}C compound; lower curve, ^{13}C compound.

erate mode (B_2 or A_1), corresponding to the vibrations on the xy plane and along the z axis, respectively. The two spectra have similar patterns in the Ni–C region, showing an intense broad band at ca. 580 cm^{-1} and a narrow band at ca. 525 cm^{-1}, assignable to the E and A/B modes, respectively (Table I). The assignment is supported by the clear shift observed in the spectra of complexes selectively labeled by ^{13}C at the carbide (Figures 1 and 2). The A/B bands are covered by the strong Ni–C–O absorptions, but their positions are revealed by a careful spectrum subtraction. The approximate force constant value (84 N m^{-1} in both cases) gives a remarkably good fit between the observed and calculated frequencies: the small discrepancy in the B_2 mode can be due to the coupling with the Ni–C–O modes (Table I).

The structure of III has not yet been determined, but chemical and spectroscopic evidences suggest a μ_4-Ni-bicapped square antiprism, closely related to that of II.[14]

By comparison of the IR spectrum with the previous one, the broad absorption centered at 584 cm^{-1} may be assigned to the degenerate M–C stretching mode, whereas the other nondegenerate mode probably has a frequency value lower than 500 cm^{-1} and is hidden by the intense Ni–C–O bonds.

(b) Complex IV. The metal skeleton is a nearly regular octahedron, capped on two opposite triangular faces by Re atoms, giving an idealized D_{3d} rhombohedron. The C atom is exactly

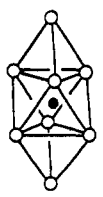

IV, V

in the center of the octahedral moiety. The vibrational modes of the interstitial C atom belong to the A_{2u} and E_u species and give rise to two medium-intensity bands in the 700–650-cm^{-1} region. The assignment is supported by ^{13}C labeling of the carbide atom, which, even if the level of labeling is not high (ca. 20%), clearly shows the expected low-frequency shift, particularly in the low-temperature spectra (Figure 3). The weak features at ca. 630 and ca. 615 cm^{-1} are probably impurity bands since they are

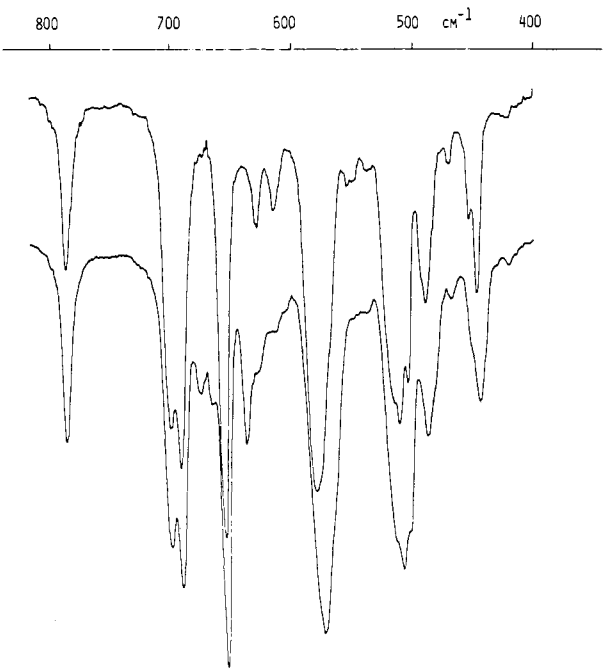

Figure 3. IR spectra of complex IV in a CsI disk at ca. 110 K: upper curve, ^{12}C compound; lower curve, ^{13}C compound.

Table II. Vibrational and Structural Data for Metal Carbide Compounds

	force const/N m^{-1}			
	f_z	f_{xy}	d_{M-C}/nm	r_C/nm[a]
$[Fe_6C(CO)_{16}]^{2-}$	200		0.189	0.056
$Co_6C(CO)_{12}S_2$	155		0.194	0.068
$[Co_6C(CO)_{15}]^{2-}$	204	235	0.195	0.068
$[Ni_8C(CO)_{16}]^{2-}$	84		0.209	0.081
$[Ni_9C(CO)_{17}]^{2-}$	84		0.209	0.081
$[Ru_6C(CO)_{16}]^{2-}$	168		0.205	0.061
$[Re_8C(CO)_{24}]^{2-}$	150	170	0.212	0.062
$[Re_7AgC(CO)_{21}]^{2-}$	145	160	0.213	0.062
$[Re_7C(CO)_{21}]^{3-}$	160	170	0.213	0.062
$[Re_7C(CO)_{21}(\mu\text{-}CO)]^{-}$	160	170	0.212	0.062
$[Re_6C(CO)_{18}(H)_2]^{2-}$	170		0.214	0.062
$[Os_{10}C(CO)_{24}]^{2-}$	200		0.204	0.060

[a] Calculated as $d_{M-C}(\text{mean}) - {}^1/_2 d_{M-M}(\text{mean})$ (see ref 3).

isotopically unshifted and, moreover, their relative intensities are different on changing the countercation. The E mode is assigned to the high-frequency band, which is broad and more intense at room temperature and split in two components as low temperature.

An SVFF calculation including a single Re–C stretching force constant does not satisfactorily account for the observed frequencies, since the expected ratio $\nu(A_{2u})/\nu(E_u)$ should be close to 1, whereas the experimental value is ca. 0.89. Introduction of interaction force constants between stretching of the Re–C bonds does not improve the calculation, because the interaction constants have identical effects on both frequencies (trans constant) or no effect at all (cis constant). Moreover, if a second force constant is introduced between the carbon and the two capping Re atoms, its calculated value (ca. −13 N m^{-1}) is physically unacceptable.

The only reliable approximation is to formulate the interstitial carbon force field in terms of axial f_z (along the C_3 axis) and equatorial f_{xy} force constants, which are related to the A_{2u} and E_u modes, respectively (Table II). On this basis, the agreement between the observed and calculated ^{13}C frequency values is remarkably good (Table I).

(c) Complexes V and VI. The structure of V actually consists of two Re_7Ag moieties joined through a Br atom interaction with the two Ag atoms.[16] The structure of one of the two independent cluster units is close to that of IV, in which one capping Re atom is substituted by an Ag atom. The metal core of complex VI is

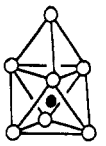

VI, VII

a monocapped octahedron, formally derived from IV by removal of a capping Re. The effect of the different capping situation introduces some distortions in the metal frame containing the carbido atom, which is no longer a regular octahedron, because the Re–Re distances in the Re_3 triangle capped by the Re atom are shorter than those in the opposite Re_3 triangle. The idealized symmetry of both clusters can be taken as C_{3v}, even if in complex VI the two opposite triangles are not perfectly staggered, giving an actual C_3 symmetry.

In both cases, the ν(Re–C) modes should give rise to a nondegenerate A_1 and a degenerate E mode, which appear as a pair of bands in the 700–600-cm^{-1} region. The one at higher frequency, probably the E mode, is broader and stronger and shows an incipient splitting in the low-temperature spectra (Figures 4 and 5).

The spectra of the ^{13}C carbide labeled complex VI support the assignment: accidental overlap of the ^{12}C A_1 mode and ^{13}C E mode is recognized by comparing the relevant intensities of the bands.

As in the previous case, the splitting between the E and A_1 bands is too large to be simply ascribed to the geometry of the clusters: on the basis of the **G** matrix only a difference $\Delta(\nu_E - \nu_{A_1})$ of 7 (VI) and 9 cm^{-1} (V) can be calculated, whereas the experimental values are 26 and 43 cm^{-1}, respectively. It is therefore straightforward to assume that two force constants are operating on the carbide atom: one along the threefold axis and the other on the plane perpendicular to it. Their values are easily calculated (Table II) and account for the experimental frequency values (Table I).

(d) Complex VII. The structure of the metal core of the complex VII is better understood if it is compared with that of complex VI. The most significant difference is the presence of a CO group bridging one edge of the Re_3 triangle opposite to the one capped by Re atom. The bridged Re–Re distance is clearly shorter than the others of the triangle, which leads to a general distortion of the metal frame in such a way that the unique remaining symmetry element is a mirror plane passing through the bridging CO, the carbide atom, and the capping Re atom.[18] The C_s symmetry requires three ν(Re–C) modes (2 A′ + A″), which appear as a broad band at room temperature; this band, however, splits into three components in the low-temperature spectrum (Figure 6). If the core structure of VII is considered a distortion of that of VI, the lowering of the symmetry from C_{3v} to C_s leads the E mode being split into A′ and A″ modes (A_1 mode (C_{3v}) becomes A′ mode (C_s)). On this basis and by comparison of the pattern of the bands with that of VI, a reasonable assignment is the following one: 695 cm^{-1} (E-derived A′ mode), 685 cm^{-1} (E-derived A″ mode), 670 cm^{-1} (A_1-derived A′ mode).

A unique Re–C stretching force constant in a SVFF gives rise to a poor fit (±10 cm^{-1}) between calculated and observed frequencies. As previously indicated, two force constants, axial and equatorial, are required to get a good fit. Their values are reported in Table II.

(e) Complexes VIII and IX. Both complexes show an approximate octahedral Re_6 arrangement around the carbon atom, but whereas complex VIII maintains a certain octahedron-derived symmetry (point group D_3),[19] complex IX is completely unsymmetric, the Re–Re distances being significantly different from each

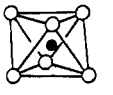

VIII, IX

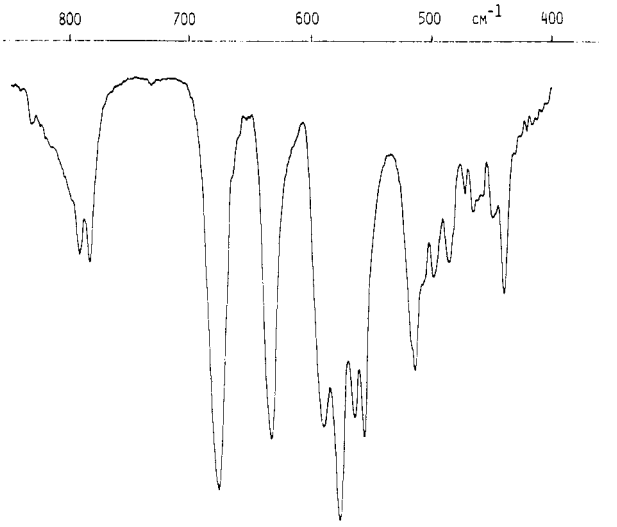

Figure 4. IR spectrum of complex V in a CsI disk at ca. 110 K.

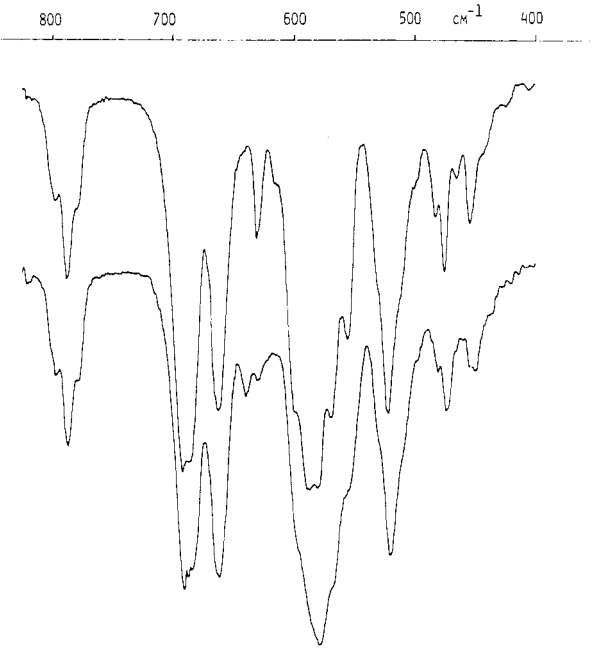

Figure 5. IR spectra of complex VI in a CsI disk at ca. 110 K: upper curve, ^{12}C compound; lower curve, ^{13}C compound.

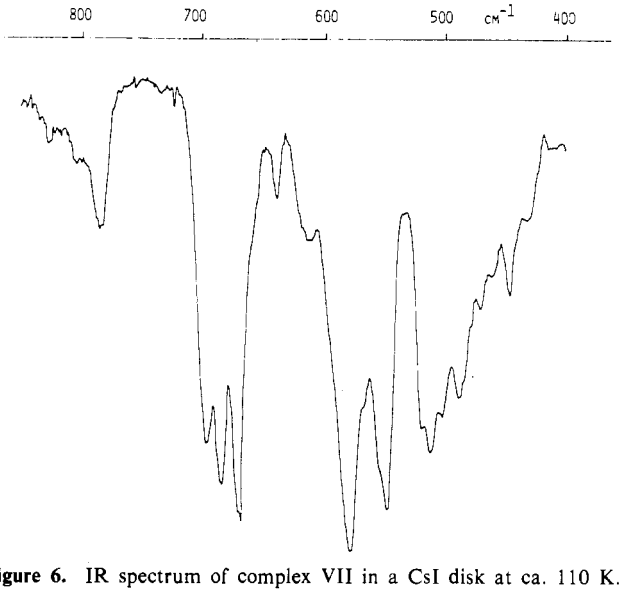

Figure 6. IR spectrum of complex VII in a CsI disk at ca. 110 K.

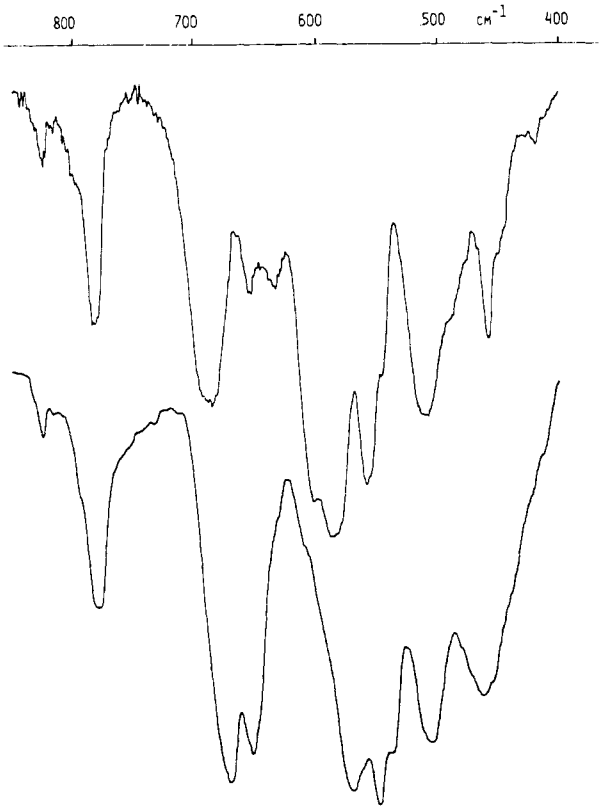

Figure 7. IR spectra of complex VIII (upper curve) and of complex IX (lower curve) in a CsI disk at ca. 110 K.

other. Moreover, the unit cell contains two crystallographically independent molecules.[18] The spectrum of complex VIII shows a large broad band at ca. 690 cm^{-1}, attributable to the ν(Re–C) modes, which remains unshifted at low temperature (Figure 7). The descent of symmetry from O_h to D_3 removes the degenerancy of the T_{1u} mode into A_2 and E modes, but the deformation is too small to allow a significant separation between them (the calculated splitting is less than 1 cm^{-1}). The spectrum of complex IX exhibits a broad band that is split into two bands at low temperature (Figure 7). The absence of any symmetry and the presence of two different molecular species do not allow reasonable interpretation of the spectral data.

Discussion

Since M–C (carbide) vibrations have frequencies comparable to those of the M–CO stretching and deformation modes, a certain extent of vibrational coupling is expected. In principle, therefore, the carbonyl ligands and their symmetry should be taken into account in calculations. Their inclusion overwhelmingly complicates the calculations, whereas their complete neglect allows the use of a simple vibrational model (see Experimental Part), which is commonly adopted[5,7,10] and seems to provide reasonable results (Table I). The model, in which the pattern of the interstitial atom vibrations depends mainly on the G matrix, allows one, mutatis mutandis, to infer structural information from the frequency values. In a square antiprismatic cage the value of the ratio between the frequencies of the vibration along the axis and the vibration in the xy plane is easily calculated as equal to h/l in which h is the height of the cage and l the side of the base. Accordingly, the relevant values are 0.903 and 0.913 for I and 0.897 and 0.900 for II. For complex III, $h/l \leq 0.85$ may be predicted on the basis of a presumable value of the frequency ratio; that is, the capping atoms cause the cage to be more flattened. The same trend has been recognized in the monocapped and bicapped square-antiprismatic clusters of Rh carbonyls containing an interstitial P atom.[21,22]

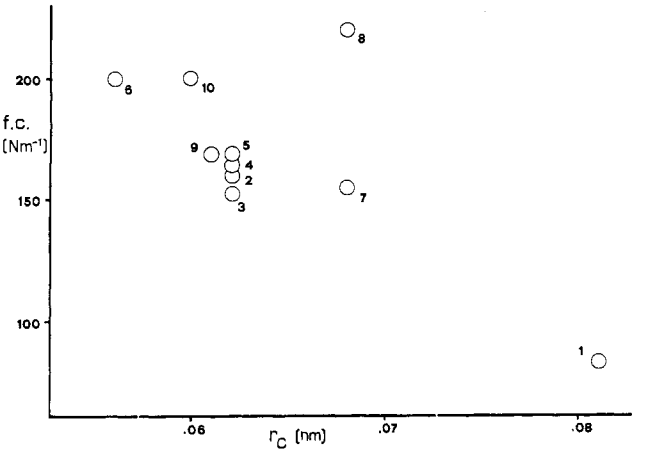

Figure 8. Plot of the average value of the M–C stretching force constant vs. covalent radius of the interstitial carbide: (1) $[Ni_8C(CO)_{16}]^{2-}$ and $[Ni_9C(CO)_{17}]^{2-}$; (2) $[Re_8C(CO)_{24}]^{2-}$ and $[Re_7C(CO)_{21}]^{3-}$; (3) $[Re_7AgC(CO)_{21}]^{2-}$; (4) $[Re_7C(CO)_{21}(CO)]^{2-}$; (5) $[Re_6C(CO)_{18}(H)_2]^{2-}$; (6) $[Fe_6C(CO)_{16}]^{2-}$; (7) $Co_6C(CO)_{12}S_2$; (8) $[Co_6C(CO)_{15}]^{2-}$; (9) $[Ru_6C(CO)_{16}]^{2-}$; (10) $[Os_{10}C(CO)_{24}]^{2-}$.

The main problem arises with the capped octahedra IV–VII. In these clusters it must be assumed that the force field associated with the carbon atom consists of two slightly different forces, one axial, f_z, operating along the threefold axis, and the other one, equatorial, f_{xy}, in the perpendicular plane. The latter is always a little larger than the former. This means that the carbide atom is subject to a lower restoring force when it vibrates along the z axis, i.e. in the direction of the capping atoms, than when it vibrates in the transversal plane. The effect can be explained in terms of different bonding interactions between p orbitals of the carbon atom and the metal orbitals centered in each triangular face of the octahedral cage. In other words, in the capped triangle the tricentric M–M interaction lying on the plane is modified by the interaction with the orbitals of the capping atom and, presumably, the orbital overlap is shifted to the center of the tetrahedron. It is reasonable that the interaction of the quadricentric MO with the carbon p_z is decreased and therefore the associate restoring force is decreased. The effect is great, when two capping atoms operate simultaneously, as the f_z values confirm (Table II).

An indirect confirmation of the "capping-atom effect" is its absence in noncapped Re systems; moreover, in complex VIII the bridging H atoms could share electron density by moving around the metal cage.

A problem arises with complex II, in which the capping effect is clearly absent, because one force constant fits the experimental data satisfactorily. Presumably, the homogeneous distribution of the electronic charge around the metal core is achieved by the large number of doubly and triply bridging CO groups, connecting in particular the apical atom with the antiprism.[14] Judging from the vibrational data, a similar pattern of CO bridges is expected with complex III, but this must be confirmed by the structural data.

In general, the capping-atom effect can be roughly measured by the extent of the splitting between ν(E) and ν(A) or by the ratio of the two force constants. More precisely, the splitting between the two frequencies is largely but not completely due to the electronic effect; a minor contribution is given by a structural effect, i.e. the geometric deformation of the octahedral cage containing the C atom. The two effects can be separately calculated by the relationship

$$\rho_{tot} = \frac{(\nu_A)_{obsd}^2}{(\nu_E)_{obsd}^2} = \frac{f_z}{f_{xy}} = \rho_{el}\rho_{str}$$

in which the total splitting factor ρ_{tot} (obviously equal to 1 in the

(21) Vidal, J. L.; Walker, W. E.; Pruett, R. L.; Schoening, R. C. *Inorg. Chem.* **1979**, *18*, 129.

(22) Vidal, J. L.; Walker, W. E.; Schoening, R. C. *Inorg. Chem.* **1981**, *20*, 238.

Table III. Values of the ρ Factors

	ρ_{tot}	ρ_{str}	ρ_{el}
$[Ni_9C(CO)_{17}]^{2-}$	0.80	0.81	0.99
$[Re_8C(CO)_{24}]^{2-}$	0.89	1.01	0.88
$[Re_7AgC(CO)_{22}]^{2-}$	0.88	0.97	0.90
$[Re_7C(CO)_{21}]^{3-}$	0.93	0.98	0.95
$[Re_7C(CO)_{21}(\mu\text{-}CO)]^{-}$	0.94	1.00	0.94
$[Re_6C(CO)_{18}(H)_2]^{2-}$	1.00	1.00	1.00

case of perfect octahedral symmetry) is a combination of a factor measuring the electronic effect ρ_{el} and of a factor measuring the structural effect ρ_{str}. The factorization of ρ_{tot} is justified by the fact that ρ_{el} can be related to the F matrix and ρ_{str} to the G matrix. ρ_{str} is easily calculated from

$$\rho_{str} = (\nu_A)_{calcd}^2/(\nu_E)_{calcd}^2$$

in which $(\nu_A)_{calcd}$ and $(\nu_E)_{calcd}$ are the best fitting values, assuming that a unique force constant is operating.

The values of the three ρ factors are reported in Table III and clearly indicate that the most important role is played by ρ_{str} in the capped Ni complex and by ρ_{el} in the capped Re complexes.

The rationalization of the ρ values in term of molecular data of the complexes is not straightforward. Obviously, ρ_{el} varies with the number of capping atoms from ca. 0.9 (two capping atoms) to ca. 0.95 (one capping atom) to 1 (no capping atom). In this context Ag and the $Re(CO)_3$ group seem to have the same electronic effect and there is no dependence on the total free anionic charge.

A clearer relationship is found between the approximate values of the M-C force constant and the relevant structural data. When the data for the complexes are separated according to the transition series of the metal, the general trend is the greater the M-C distance, the smaller the force constant (Table II).

A plot of the apparent radius of the carbide atom r_C vs. the force constant (Figure 8) provides a general illustration of the above trend. A progressive decrease of force constant on increasing r_c is apparent, regardless of the metal transition series and the approximation adopted in calculating the force constant. These results suggest that there will be a decrease of the interaction of the carbide atom with the metals when the size of the metal cavity is increased.

Acknowledgment. We thank the Italian MPI for financial support.

Registry No. I, 85190-60-9; II, 90051-77-7; III, 93756-02-6; IV, 83267-47-4; V, 99704-71-9; VI, 83351-85-3; VII, 109181-95-5; VIII, 85601-11-2; IX, 98938-43-3; ^3C, 14762-74-4.

Contribution from the Chemistry Department, The University of Alabama at Birmingham, Birmingham, Alabama 35294

^{13}C and ^{17}O NMR and IR Spectroscopic Study of a Series of Carbonyl(4-substituted pyridine)(*meso*-tetraphenylporphinato)iron(II) Complexes. Correlations between NMR Chemical Shifts and IR Stretching Frequencies of the Carbonyl Ligand and Taft Parameters of the Pyridine Substituent

James W. Box and Gary M. Gray*

Received September 16, 1986

The results of a ^{13}C and ^{17}O NMR and IR spectroscopic study of a series of carbonyl(4-substituted pyridine)(*meso*-tetraphenylporphinato)iron(II) (Fe(TPP)(CO)(py-4-X)) complexes are presented. Good to excellent linear correlations between the ^{13}C and ^{17}O NMR chemical shifts and the IR stretching frequencies of the carbonyl ligand are observed as the pyridine substituent is varied. Good to excellent linear correlations are also observed between these NMR chemical shifts and IR stretching frequencies and the NMR chemical shifts and IR stretching force constants for the trans carbonyls of a series of *cis*-$Mo(CO)_4(py\text{-}4\text{-}X)_2$ complexes as the pyridine substituent is varied. The relationship between the donor ability of the pyridine ligands and the ^{13}C and ^{17}O NMR chemical shifts and IR stretching frequencies of the carbonyl ligands in the Fe(TPP)(CO)(py-4-X) complexes has been quantitated by fitting the spectroscopic data to the single and the dual Taft substituent parameters of the pyridine substituent. Good to excellent correlations are observed. The upfield shift in the ^{13}C NMR resonance of the carbonyl ligand as the electron-donor ability of the pyridine increases is unique. This has been rationalized by using the Buchner and Schenk description of metal carbonyl ^{13}C NMR chemical shifts.

Introduction

Metalloproteins containing an iron-porphyrin active site have diverse biological functions, many of which involve coordination to and/or reaction with a dioxygen ligand.[1-6] The differences in the reactivity of the iron-porphyrin proteins toward dioxygen are surprising in view of the great similarities between the active sites in these proteins. It has been suggested that these differences are due, in part, to the differences in the axial ligands that are coordinated to the iron-porphyrin active site.[7]

The electron-donor ability of the axial ligand may have a significant effect on the reactivity of a dioxygen ligand coordinated to an iron-porphyrin center. As the electron-donor ability of the axial ligand increases, the electron density at the iron increases. This, in turn, should increase the donation of electron density into the π^* orbitals of an η^1-dioxygen ligand and weaken the O-O double bond, increasing the reactivity of the ligand. Unfortunately, it is difficult to study this relationship using simple iron-porphyrin complexes of dioxygen as model systems since these complexes are unstable.[8]

Carbonyl complexes of simple iron porphyrins may be an acceptable alternative to the dioxygen complexes as models for the relationship between the electron-donor ability of the axial ligand

(1) Pratt, J. H. In *Inorganic Biochemistry*; Eichhorn, G. L., Ed.; Elsevier: New York, 1975; p 832.
(2) Debrunner, P. G.; Gunsalus, I. C.; Sligar, S. G.; Wagner, G. C. In *Metal Ions in Biological Systems*; Sigel, H., Ed.; Dekker: New York, 1978; Vol. 7, Chapter 6.
(3) Wagner, G. C.; Gunsalus, I. C. In *The Biological Chemistry of Iron*; Dunford, H. B., Dolphin, D., Raymond, K. N., Sieker, L., Eds.; Reidel: Dordricht, The Netherlands, 1981; p 405.
(4) Jones, P.; Wilson, I. In *Metal Ions in Biological Systems*; Sigel, H., Ed.; Dekker: New York, 1978; Vol. 7, Chapter 5.
(5) Nichols, P.; Chance, B. In *Molecular Mechanisms of Oxygen Activation*; Hayaishi, O., Ed.; Academic: New York, 1974; p 479.
(6) Dunford, H. B.; Araiso, T.; Job, D.; Ricard, J.; Rutter, R.; Hager, L. P.; Wever, W. M.; Boelens, R.; Ellfolk, N.; Ronnberg, M. In *The Biological Chemistry of Iron*; Dunford, H. B., Dolphin, D., Raymond, K. N., Sieker, L., Eds.; Reidel: Dordrecht, The Netherlands, 1981; p 337.
(7) Hill, H. A. O. In *The Biological Chemistry of Iron*; Dunford, H. B., Dolphin, D., Raymond, K. N., Sieker, L., Eds.; Reidel: Dordrecht, The Netherlands, 1981; p 3.
(8) Reed, C. A. In *Metal Ions in Biological Systems*; Sigel, H., Ed.; Dekker: New York, 1978; Vol. 7, Chapter 7.

0020-1669/87/1326-2774$01.50/0